

# Property and Structure Characterization of High Molecular Weight Polyacrylonitrile Polymers Initiated by 2,2'-Azobis (2-methyl propionamide) Dihydrochloride Using Aqueous Deposited Polymerization Technique

Yaqi Zhao\*, Banglei Liang, Zhenxin Zhao and Qiao Feng

School of Materials and Chemical Engineering, Henan University of Urban Construction, Pingdingshan, China

**Abstract.** Powdery high molecular weight polyacrylonitrile (HMW-PAN) polymers were successfully synthesized by aqueous deposited polymerization (ADP) method with 2,2'-azobis (2-methyl propionamide) dihydrochloride (AIBA) as the initiator and itaconic acid (IA) as comonomer. The utilization of IA into the ADP system was conducive to relax the proceeding of thermo-oxidation process. Differential scanning calorimeter (DSC) curves of obtained PAN copolymers showed the doublet peaks character under air atmosphere, attributing to the exothermic cyclization and oxidative reactions during heat-treatment process. With the utilization of IA in the reaction system, crystallinity and grain sizes of the PAN polymers decreased. The stretching vibration of nitrile group ( $C\equiv N$ ) at  $2240\text{cm}^{-1}$  was the strongest peak in both Fourier transform infrared spectra (FTIR). And the stretching vibration and bending of  $\text{CH}_2$  were the stronger peaks in FTIR. Amido group ( $\text{NH}_2$ ), carbonyl group ( $\text{C}=\text{O}$ ) and C-O single bond existed in FTIR of PAN homopolymer and copolymers, indicating occurrence of  $\text{C}\equiv\text{N}$  hydrolysis during polymerization process except carboxyl group ( $\text{COOH}$ ) introduced by IA.

## 1. Introduction

High molecular weight polyacrylonitrile (HMW-PAN) copolymer is one of the best precursors to prepare high quality carbon fibers [1-3]. During the preparation process of HMW-PAN copolymers, some vinyl comonomers containing flexible functional groups have been focused by many investigators, such as acyclic acid (AA), itaconic acid (IA), methylacrylate (MA), vinyl acetate (VAc), and so on [4-10]. And their thermal properties and structural characters had a direct effect on PAN copolymer spinning dopes. Therefore, the introduction of a few comonomers greatly enhanced the internal mobility of PAN's segments, depressed the onset of cyclized temperature during oxidation, and improved the final spinnability of PAN dopes.

Compared with traditional homogeneous solution polymerization, HMW-PAN can be prepared by aqueous polymerization system, because of none chain transfer reactions and partially-solubility of acrylonitrile (AN) in water ( $\text{H}_2\text{O}$ ) system. As one kind of heterogeneous solution polymerization, there have been some reports about aqueous deposited polymerization (ADP) of AN. But many complex initiating systems containing alkali metallic ions were usually employed to initiate their copolymerizations. This is not beneficial to manufacture high quality PAN-based precursors for carbon fibers [11-15]. So it is necessary to search an appropriate initiator for the production of HMW-PAN copolymers. By now, there

have been some reports about the important water-soluble initiator ammonium persulphate with none alkali metallic ions [16-19]. But there have been few reports about the water-soluble azo initiator, which can also initiate the PAN's copolymerization through the water-soluble radical in water phase. And HMW-PAN can be also obtained using the ADP technique.

In this paper, as a single organic and water-soluble initiator without alkali metallic ions, 2,2'-azobis (2-methyl propionamide) dihydrochloride (AIBA) was used as the initiator, which is a relatively moderate initiator to control the polymerization process and thermal properties of PAN copolymers [20-22]. And a commonly used comonomer-itaconic acid (IA) was copolymerized with AN using the ADP technique. Furthermore, there are also few reports about detailed property and structure characterization of powdery HMW-PAN polymers directly obtained by this initiator. As a result, thermal properties of PAN polymers obtained were investigated by thermal analyzer. And their physical and chemical structures were discussed by wide-angle X-ray diffraction (WAXD) and Fourier transform infrared spectra (FTIR).

\* Corresponding author: zhyq5891@163.com

## 2. Experimental Section

### 2.1 Original Materials

AN (Zhengzhou Paini Chemical Reagent Factory, China) and IA (Tianjin Guangfu Fine Chemical Research Institute, China) were analytically purity used as the reaction monomers without further treatment. AIBA (Shanghai Kaiyang Biological Technology Co., Ltd, China) with 98% purity was directly used. And deionized H<sub>2</sub>O was adopted as the reaction medium during the polymerization process.

### 2.2 ADP of PAN

Powdery PAN homopolymer and PAN copolymer with different weight fractions of IA (0~10wt%) in the feed, i.e. Homo-PAN and various P(AN-co-IA)s, were synthesized under nitrogen (N<sub>2</sub>) atmosphere using a three-necked flask with deionized H<sub>2</sub>O at 60°C. The synthesized samples were described as Homo-PAN, PI-1, PI-2, PI-3, and PI-4, corresponding to 0wt%, 1wt%, 2wt%, 4wt%, 10wt% IA in the feed, respectively. While the concentration of AIBA was 1wt% based on the total monomer concentration at 22wt%. Good agitation was used to ensure that the reaction heat could be thrown off in the polymerization process. The reaction time lasted 2h. And then the precipitated products were washed successively with water and methanol, and dried to a constant weight under vacuum at 50°C.

### 2.3 Measurements

Conversions of the polymerizations were tested using weight method. Viscosity average molecular weights ( $M_v$ ) of Homo-PAN and P(AN-co-IA)s were determined by Ubbelohde viscometer method at (30±0.2)°C using dimethylsulfoxide (DMSO) solvent. The intrinsic viscosity  $[\eta]$  equation was calculated by one-point method as follows:

$$[\eta] = \frac{\sqrt{2(\eta_{sp} - \ln \eta_r)}}{c}, [\eta] = 2.865 \times 10^{-4} M_v^{0.768} \quad (1)$$

where the needed PAN weight was about 0.04–0.05g in 50mL DMSO.

TA Instruments Co. SDT Q600 (USA) thermal analyzer was used to get simultaneous thermal analysis (STA) curves of different PAN polymers, including differential scanning calorimeter (DSC) and thermal gravity analysis (TGA) curves. Their STA curves with the temperature range from room temperature to 450°C were tested at a 10°C/min heating rate under air atmosphere. Also the DSC curves under N<sub>2</sub> atmosphere were measured using PerkinElmer DSC 8500 (USA) thermal analyzer with the aluminum crucible under aluminum cover, whose temperature range was from room temperature to 400°C. Wide-angle X-ray diffraction (WAXD) of Homo-PAN and P(AN-co-IA)s between 5~50° were measured at a 3.6°/min step rate under room temperature by PANalytical X'Pert Pro analyzer (Holland) All the WAXD measurements were well done under the same conditions. Crystallinity index ( $X_c$ ) was calculated by the integral area method according the references [23–25].

And the crystalline planar spacing  $d$  and crystallite size ( $L_c$ ) were determined by Scherrer equation and Bragg equation [25, 26].

FTIR of Homo-PAN and P(AN-co-IA)s were recorded on PerkinElmer Frontier (USA) spectrometer for 16 times. The transmission mode was used on finely pure powdery samples using direct compression method without KBr. The testing range was from 400cm<sup>-1</sup> to 4000cm<sup>-1</sup>.

## 3. Results and discussions

### 3.1 Acquirement of HMW-PAN polymers

As detailed in Table 1, the  $M_v$  values measured by the method above are approximately above 16×10<sup>4</sup>. It is evidently investigated that the synthesized PAN polymers almost had the higher molecular weights than the results in the references [12,13,26]. The main reason is that H<sub>2</sub>O was adopted as reaction medium in ADP process. Due to the presence of H<sub>2</sub>O, chain transfer reactions were prevented, which could increase average molar weights of PAN polymers. While in the homogeneous solution polymerization process of AN and vinyl comonomers, chain transfer reactions to reaction solvents, such as DMSO, dimethylformamide (DMF) and so on, would lower molecular weights of the final PAN copolymers [12,13,26]. Furthermore, relative researches and monomer reactivity ratios of AN and IA have been reported by Zhao et al [16,17], which is deduced that the IA comonomer has the higher reactivity than AN monomer. So, the samples PI-1 and PI-2 with 1wt% and 2wt% IA in the feed had the higher  $M_v$  values than the Homo-PAN. When the IA amount reached 4wt%, the IA amount in the PAN main chains became much more enough to prevent the active chain growth. And the  $M_v$  value of sample PI-3 became lower. While the conversions of samples PI-2 and PI-3 had become higher than samples Homo-PAN and PI-1. However, only the 14.09% products were prepared with its  $M_v$  value at 16.18×10<sup>4</sup> about sample PI-4 copolymer with 10wt% IA. Thus, more IA comonomer in the feed was not conducive to produce HMW-PAN copolymer with high conversion.

**Table 1.** ADP results of AN/IA under different monomer ratios

Samples	AN/IA(w/w)	Conversion (%)	$M_v$ (×10 <sup>4</sup> )
Homo-PAN	100/0	76.39	40.60
PI-1	99/1	66.10	55.94
PI-2	98/2	82.91	52.93
PI-3	96/4	83.12	41.74
PI-4	90/10	14.09	16.18

### 3.2 STA Analysis of PAN Polymers

Different DSC curves of powdery Homo-PAN and different P(AN-co-IA)s under air and N<sub>2</sub> atmosphere are listed in Figure 1(a) and Figure 1(b). The parameters obtained from the exotherms including the initiation temperature ( $T_i$ , the temperature when the exothermic reactions begin), the termination temperature, i.e., the

final temperature ( $T_f$ , the temperature when the exothermic reactions end), their difference ( $\Delta T = T_f - T_i$ ), the exothermic peak temperature ( $T_p$ , the evident exothermic peak in DSC curves), the evolved heat ( $\Delta H$ ) and the velocity of evolving heat ( $\Delta H/\Delta T$ ) are described in Table 2.

DSC exotherms of different PAN polymers are due to the oxidative reactions and cyclization reactions under different atmospheres [1-3, 13]. The obtained exotherm parameters also reflect different reaction characters. The  $T_i$  values for all the P(AN-co-IA)s were much smaller than Homo-PAN, indicating that a greater release of the exothermic initiation process with IA in the feed.  $T_i$  values showed a change tendency to become lower with the increase of required IA amounts in the polymerization system. It can be concluded that IA played a significant role in initiating the exothermic reaction of different PAN copolymers. However, the  $T_p$  and  $T_f$  values showed few changes, indicating that  $T_p$  and  $T_f$  were not greatly affected by the increase of the IA comonomer [1-3, 13, 16, 25-27].

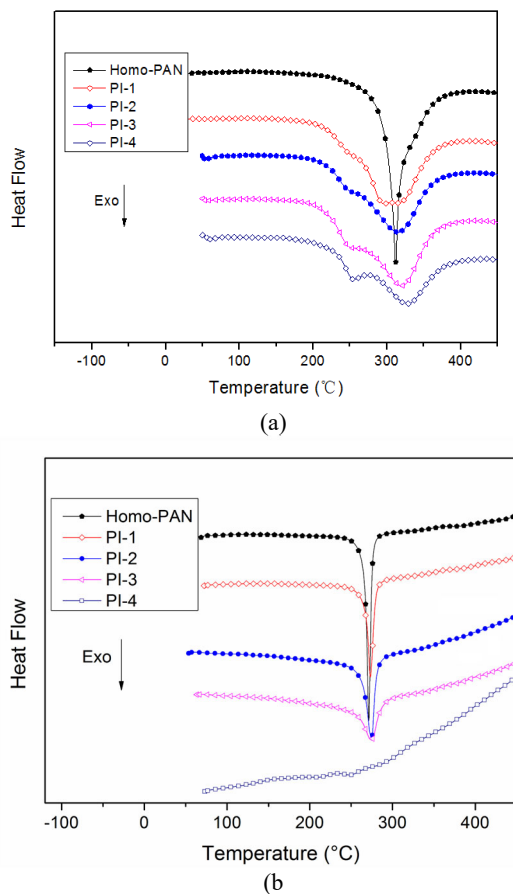


**Figure 1.** DSC curves of Homo-PAN and different P(AN-co-IA)s under air atmosphere from STA results and DSC curves of Homo-PAN and different P(AN-co-IA)s under N<sub>2</sub> atmosphere

**Table 2.** Parameters of DSC curves of Homo-PAN and different P(AN-co-IA)s

samples	atmosphere	$T_i$ (°C)	$T_p$ (°C)	$T_f$ (°C)	$\Delta T$ (°C)	$\Delta H$ (J·g <sup>-1</sup> )	$\frac{\Delta H}{\Delta T}$ (J·g <sup>-1</sup> ·°C <sup>-1</sup> )
Homo-PAN	Air	220	312	375	155	4194	27.06
PI-1		212	315	377	165	4303	26.08
PI-2		206	317	380	174	4968	28.55
PI-3		199	249,319	385	186	4920	26.45
PI-4		187	255,327	389	202	3917	19.39
Homo-PAN	N <sub>2</sub>	267	271	275	8	445	55.63
PI-1		268	273	280	12	418	34.83
PI-2		264	274	281	17	353	20.76
PI-3		260	276	285	25	231	9.24
PI-4		237	251	310	83	220	2.65

Another phenomenon deduced from DSC curves was the doublet peaks character in different P(AN-co-IA)s under air atmosphere. While in case of Homo-PAN, the doublet character was not very clear. It could be relevant to the different reaction mechanism during heat-treatment process of different PAN polymers. Furthermore, with the increase of IA amounts, much more intricate changes were found in DSC exotherms of different P(AN-co-IA)s, which was probably due to the superposition of the two peaks. The doublet peaks might be due to the exothermic cyclization and oxidative reactions during heat-treatment process. And the reactions might happen more or less simultaneously. However, initiation of oxidation reaction occurred before the onset of cyclization. The lower-temperature exothermic peak was attributed to the primary oxidation (including dehydrogenation) and cyclization reactions. And the higher-temperature exothermic peak was attributed to the secondary oxidation reactions leading to the polymer chain scission. The evolution of HCN, CO<sub>2</sub> and CO also happened in this region. There is no essential difference to the experimental results by the other many workers [13, 28-30].

While in the N<sub>2</sub> atmosphere, the different PAN polymers had higher  $T_i$  values, lower  $T_f$ ,  $T_p$ ,  $\Delta T$  and  $\Delta H$  values than those in air atmosphere. The main reason was due to strong oxidation reactions under air atmosphere of different PAN polymers. In addition, the Homo-PAN had the minimum  $\Delta T$  and the maximum  $\Delta H/\Delta T$ . At the same time, the broader (higher  $\Delta T$ ) and the smoother (lower  $\Delta H/\Delta T$ ) exotherm were found in different PAN copolymer than in Homo-PAN. It is indicated that the evolving heat was concentrative and expeditious in Homo-PAN. The IA comonomer slowed the rate of exothermic reaction. It is obvious that the IA comonomer has role of relieving exothermic reactions of PAN polymers.

### 3.3 TGA Analysis of PAN Polymers

TGA curves of powdery Homo-PAN and different P(AN-co-IA)s are shown in Figure 2. Obviously, weight loss reactions of all PAN polymers included three reaction stages, named as micro-scale weight loss zone, intense weight loss zone and slow weight loss zone, which were related to small molecules loss and intense exothermic reactions. And the three stages were combined into the preoxidation process of PAN-based precursors, whose

difference reflected the different degree and rate of the preoxidation reaction. According to the TGA curves, the initiation decomposition temperature ( $T_{id}$ ) and different weight loss values obtained from the TGA curves including  $w_1$  (%),  $w_2$  (%) and  $w_3$  (%) corresponding to the three stages were listed in Table 3.

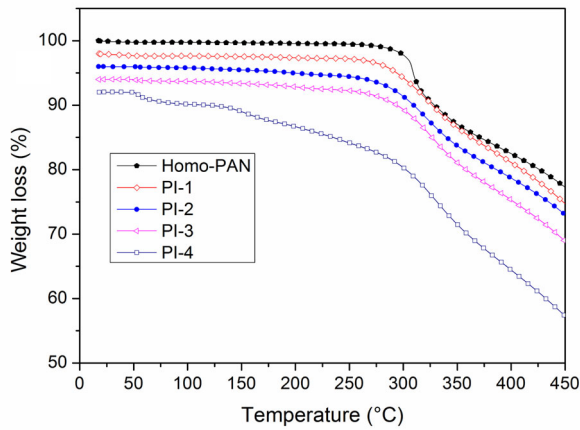


**Figure 2.** TGA curves of Homo-PAN and different P(AN-co-IA)s under air atmosphere from STA results

**Table 3.** Parameters for TGA curves of Homo-PAN and different P(AN-co-IA)s

Samples	$T_{id}$ (°C)	$w_1$ (%)	$w_2$ (%)	$w_3$ (%)
Homo-PAN	303	0.5	12.9	22.3
PI-1	282	0.7	11.4	23.3
PI-2	277	1.1	11.5	23.0
PI-3	275	1.2	13.7	25.1
PI-4	132	1.7	10.3	34.5

It is investigated that the first stage occurred at the higher temperature to the Homo-PAN with none IA, with its largest weight loss slope seen from Figure 2. All P(AN-co-IA)s had ease exothermic reactions under air atmosphere, with its lower  $T_{id}$  values. When the IA amount was less than 4wt%, the  $w_1$  and  $w_3$  weight loss values had low rise trend. Due to the introduction of IA comonomer in the feed, the increase of  $w_1$ ,  $w_2$  and  $w_3$  were attributed to higher IA content in the PAN main chains, which might promote the pyrolysis reaction. At the same time, when the IA amount reached 10wt%, the  $w_1$  and  $w_3$  reached the maximum values. That is to say, sample PI-4 had much more weight loss at the first and third stage. However, the sample PI-3 had the higher  $w_2$  value and the sample PI-4 with the lowest  $w_2$  value. Higher IA content in sample PI-3 was benefit to the exothermic reaction, which made the  $w_2$  value become higher. While the  $T_{id}$  value of sample PI-4 was so lower that it made the exothermic reaction occurred much more early. And the sample PI-4 also had the lowest  $M_v$  value. Therefore, the  $w_2$  value became a little smaller. It was probably attributed to interactive affect of higher IA contents in the final P(AN-co-IA) polymers and their  $M_v$  values [1-3, 13, 25-30].

### 3.4 WAXD Analysis of PAN Polymers

WAXD curves of Homo-PAN and different P(AN-co-IA)s measured under room temperature are depicted in Figure 3. It is shown that all the PAN polymers had the strongest diffraction peaks appearing at  $2\theta$  around  $17^\circ$ . They were corresponded to (100) crystalline plane of the pseudo-hexagonal cell or (200) reflections of the orthorhombic structure with their  $d$  values equaling about 0.53nm [31-33]. It is noticed that the centers of the strongest diffraction peaks hardly changed with the increase of required IA amounts. Therefore,  $d$  values of different PAN polymers basically remained unchanged. But the changes of peak intensity and peak area caused changes of crystallinity in different PAN polymers.

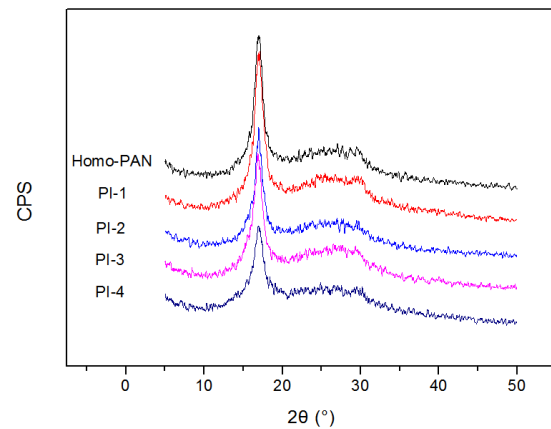


**Figure 3.** WAXD curves of Homo-PAN and different P(AN-co-IA)s

Then all the  $d$ ,  $L_c$  and  $X_c$  values can be deduced and listed in Table 4. It is seen that the Homo-PAN with none IA in the feed had the best crystallinity than the other PAN copolymers under room temperature, which was relevant to destructive effect of introduced IA comonomer. And the destructive effect became larger with the increase of IA less than 4wt%. Fewer orderly arrangement zones were acquired in the P(AN-co-IA)s, which would decrease their crystallinity and grain sizes. Therefore, the sample PI-4 with the highest IA content had the lowest  $L_c$  and  $X_c$  values.

**Table 4.** Parameters for WAXD curves of Homo-PAN and different P(AN-co-IA)s

Samples	$2\theta$ (°)	$d$ (nm)	FWHM (°)	$L_c$ (nm)	$X_c$ (%)
Homo-PAN	16.92	0.524	1.298	6.125	53.1
PI-1	17.10	0.519	1.272	6.251	48.9
PI-2	16.98	0.522	1.270	6.260	48.0
PI-3	16.95	0.523	1.273	6.245	47.5
PI-4	16.98	0.522	1.409	5.642	43.3

### 3.5 FTIR Analysis of PAN Polymers

FTIR of powdery Homo-PAN and P(AN-co-IA)s are described in Figure 4. It is obvious that the stretching vibration ( $\nu$ ) of nitrile group ( $C\equiv N$ ) at  $2240\text{ cm}^{-1}$  was the

strongest peak in FTIR spectra. And the 2240  $\text{cm}^{-1}$  band remained unchanged in the Homo-PAN and P(AN-co-IA)s. It is indicated that the AN units appeared the status of uninterrupted long sequences [34]. A shoulder-like absorption peak around 2190  $\text{cm}^{-1}$  near the  $\text{C}\equiv\text{N}$  group might be due to the  $\nu\text{C}=\text{NH}$  formed during the ADP process [35]. Besides, the stretching vibration around 2940 $\text{cm}^{-1}$  and bending vibration ( $\delta$ ) around 1450 $\text{cm}^{-1}$  of methylene group ( $\text{CH}_2$ ) were the stronger peak in the two spectra. During ADP of AN and IA,  $\text{C}\equiv\text{N}$  would be changed into amide group ( $\text{CONH}_2$ ) or carboxyl group ( $\text{COOH}$ ) owing to hydrolysis under water bath heating [28,36]. Thus, a double broad absorption peak at 3628 $\text{cm}^{-1}$  and 3546 $\text{cm}^{-1}$  belonging to stretching vibration of  $\text{NH}_2$  and a weak absorption peak at 1621 $\text{cm}^{-1}$  belonging to bending vibration of  $\text{NH}_2$  could be exhibited in FTIR of Homo-PAN and P(AN-co-IA)s. Simultaneously, a weak and broad band at 3248 $\text{cm}^{-1}$  might belong to double-frequency band of  $\delta\text{NH}_2$  (DFB- $\delta\text{NH}_2$ ) at 1624 $\text{cm}^{-1}$ .

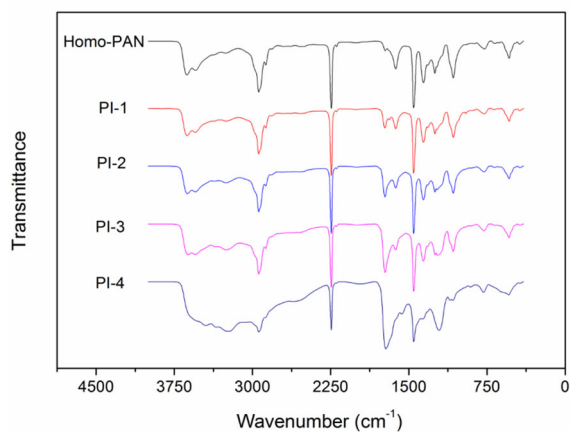


**Figure 4.** FTIR of Homo-PAN and different P(AN-co-IA)s

Furthermore, a weak absorption peak at 1735 $\text{cm}^{-1}$  presented in Homo-PAN was possibly attributed to carbonyl group ( $\text{C}=\text{O}$ ) formed in hydrolysis process. Compared to Homo-PAN, the absorption band around 1735 $\text{cm}^{-1}$  in P(AN-co-IA) was stronger than Homo-PAN because IA is a carboxyl compound, which includes two carboxyl groups in one molecule. As a result of the two reasons above, the intensity of  $\nu\text{C}=\text{O}$  is stronger than that of  $\delta\text{NH}_2$ . The weak stretching vibration of hydroxyl group ( $\text{OH}$ ) was superposed to DFB- $\delta\text{NH}_2$  at 3248 $\text{cm}^{-1}$ . So the absorption band at 3248 $\text{cm}^{-1}$  in P(AN-co-IA)s was a little stronger than that in Homo-PAN. The C-H vibrations of different modes were shown in the band regions at 1370~1350 $\text{cm}^{-1}$  and 1270~1220 $\text{cm}^{-1}$  [35]. It is reported by Minagawa et al that the stereospecific absorption bands at 1250 and 1230 $\text{cm}^{-1}$  might be assigned to the wagging mode of the C-H group coupled with rocking mode of the  $\text{CH}_2$  group[37]. Due to excess hydrolysis of the  $\text{C}\equiv\text{N}$  group, an indistinct absorption band around 1180 $\text{cm}^{-1}$  might be assigned to  $\nu\text{C}-\text{O}$  bond.

## 4. Conclusion

Powdery HMW-PAN polymers were synthesized by ADP technique using AIBA as initiator. According to investigations of thermal properties and structure characters using TA, WAXD and FTIR, some conclusions can be obtained as follows:

The different PAN polymers synthesized had the higher molecular weights and higher conversions with the required IA amounts at 1wt%, 2wt% and 4wt%.

The use of IA into the polymerization system was available for relaxing the thermooxidation process of different PAN copolymers. Simultaneously, DSC curves of the PAN copolymers under air atmosphere revealed the doublet peaks phenomenon, which was not evident in Homo-PAN and in  $\text{N}_2$  atmosphere. And TGA curves of the PAN polymers were divided into three stages. More IA used in the ADP system made the P(AN-co-IA)s have lower initiation decomposition temperature and larger loss weight value.

(3) IA in the feed caused destructive effect to the crystal structure of PAN polymers, which made the crystallinity and grain sizes of the PAN polymers decrease. The nitrile group ( $\text{C}\equiv\text{N}$ ) stretching vibration at 2240 $\text{cm}^{-1}$  and stretching vibration and bending of  $\text{CH}_2$  were very strong in both FTIR. In Homo-PAN, a weak absorption at 1730 $\text{cm}^{-1}$  was attributed to the  $\text{C}=\text{O}$  group stretching vibration because of hydrolysis of  $\text{C}\equiv\text{N}$ . However, it became stronger in different P(AN-co-IA)s with the increase of required IA dosages in the feed.

## Acknowledgments

This work was financially supported by the fund of National Science Foundation of China (Grant No. 51803047), and the fund of Science and Technology Key Project of Henan Province in China (Grant No. 202102210035), and the fund of Young Key Teachers Cultivating Program of Henan Province Universities in China (Grant No. 2019GGJS227), and the fund of Academic Technology Leader Program of Henan University of Urban Construction (Grant No. YCJXSJSDTR201909).

## References

1. A.K. Gupta, D.K. Paliwal, P. Bajaj, Acrylic precursors for carbon fibers, *J. Macromol. Sci. R. M. C.* 31 (1991) 1-89.
2. K. Sen, S.H. Bahrmi, P. Bajaj, High performance acrylic fibers, *J. Macromol. Sci. R. M. C.* 36 (1996) 1-76.
3. P. Bajaj, A.K. Roopanwal, Thermal stabilization of acrylic precursors for the production of carbon fibers: an overview, *J. Macromol. Sci. R. M. C.* 37 (1996) 97-147.
4. G.H. Olive, S. Olive, The chemistry of carbon fiber formation from polyacrylonitrile, *Adv. Polym. Sci.* 51 (1983) 1-60.

5. W.J. Howard. The glass temperatures of polyacrylonitrile and acrylonitrile-vinyl acetate copolymers, *J. Appl. Polym. Sci.* 5 (1961) 303-307.
6. M.M. Coleman and G.T. Sivy, Fourier transform IR studies of the degradation of polyacrylonitrile copolymers-I: Introduction and comparative rates of the degradation of three copolymers below 200°C and under reduced pressure, *Carbon* 19 (1981) 123-126.
7. G.T. Sivy, M.M. Coleman, Fourier transform IR studies of the degradation of polyacrylonitrile copolymers-II: Acrylonitrile/methacrylic acid copolymers, *Carbon* 19 (1981) 127-131.
8. M.M. Coleman, G.T. Sivy, Fourier transform IR studies of the degradation of polyacrylonitrile copolymers-III: Acrylonitrile/vinyl acetate copolymers, *Carbon* 19 (1981) 133-135.
9. G.T. Sivy, M.M. Coleman, Fourier transform IR studies of the degradation of polyacrylonitrile copolymers-IV: acrylonitrile/acrylamide copolymers, *Carbon* 19 (1981) 137-139.
10. J.S. Tsai, C.H. Lin, Effect of comonomer composition on the properties of polyacrylonitrile precursor and resulting carbon fiber, *J. Appl. Polym. Sci.* 43 (1991) 679-685.
11. A. Maity, M. Biswas, Kinetics and mechanism of the K<sub>2</sub>CrO<sub>4</sub>-NaAsO<sub>2</sub> redox-initiated aqueous polymerization of acrylonitrile, *J. Appl. Polym. Sci.* 96 (2005) 276-280.
12. P. Bajaj, D.K. Paliwal, A.K. Gupta, Acrylonitrile-acrylic acids copolymers. 1. Synthesis and characterization, *J. Appl. Polym. Sci.* 49 (1993) 823-833.
13. A.K. Gupta, D.K. Paliwal, P. Bajaj, Effect of the nature and mole fraction of acidic comonomer on the stabilization of polyacrylonitrile, *J. Appl. Polym. Sci.* 59 (1996) 1819-1826.
14. J.R. Ebdon, T.N. Huckerby, T.C. Hunter, Free-radical aqueous slurry polymerizations of acrylonitrile: 1. End-groups and other minor structures in polyacrylonitriles initiated by ammonium persulfate/sodium metabisulfite, *Polymer* 35 (1994) 250-256.
15. J.R. Ebdon, T.N. Huckerby, T.C. Hunter, Free-radical aqueous slurry polymerizations of acrylonitrile: 2. End-groups and other minor structures in polyacrylonitriles initiated by potassium persulfate/sodium bisulfite, *Polymer* 35 (1994) 4659-4664.
16. Y.Q. Zhao, C.G. Wang, Y.X. Wang, B. Zhu, Aqueous deposited copolymerization of acrylonitrile and itaconic acid, *J. Appl. Polym. Sci.* 111 (2009) 3163-3169.
17. Y.Q. Zhao, C.G. Wang, M.J. Yu, C.S. Cui, Q.F. Wang, B. Zhu, Study in monomer reactivity ratios of acrylonitrile/itaconic acid in aqueous deposited copolymerization system initiated by ammonium persulfate, *J. Polym. Res.* 16 (2009) 437-442.
18. C.S. Cui, C.G. Wang, Y.Q. Zhao. Acrylonitrile/ammonium itaconate aqueous deposited copolymerization, *J. Appl. Polym. Sci.* 102 (2006) 904-908.
19. C.S. Cui, C.G. Wang, Y.Q. Zhao. Monomer reactivity ratios for acrylonitrile-ammonium itaconate during aqueous-deposited copolymerization initiated by ammonium persulfate, *J. Appl. Polym. Sci.* 100 (2005) 4645-4648.
20. J.P. Liu, X.M. Yang, X.F. Hu, L. Hu, Recent research progress on the synthesis and application of water soluble azo initiators, *Chemical Reagents*, 33 (2001) 317-323.
21. S.S. Wang, Y.S. Chen, Q. Ouyang, J. Huang, J.X. Yang, H. Liu, Y.F. Liu, Effect of azo initiators on structure and thermal stabilization behavior of PAN and its precursor, *China Synthetic Fiber Industry*, 40 (2017) 11-16.
22. Z.H. Xie, Y.S. Chen, Q. Ouyang, X.F. Wang, J.X. Yang, J. Huang, Study on acrylonitrile solution polymerization initiated by azobiscyanopentanoic acid, *China Synthetic Fiber Industry*, 38 (2015) 13-17.
23. J.P. Bell, J.H. Dumbleton, Changes in the structure of wet-spun acrylic fibers during processing, *Text. Res. J.* 41 (1971) 196-203.
24. G. Hinrichsen, Structural changes of drawn polyacrylonitrile during annealing, *J. Polym. Sci. Polym. Symp.* 38 (1972) 303-319.
25. A.K. Gupta, R.P. Singhal, Effect of copolymerization and heat treatment on the structure and X-ray diffraction of polyacrylonitrile, *J. Polym. Sci. Polym. Phys.* 21 (1983) 2243-2262.
26. P. Bajaj, K. Sen, S.H. Bahrmil, Solution polymerization of acrylonitrile with vinyl acids in dimethylformamide, *J. Appl. Polym. Sci.* 59 (1996) 1539-1550.
27. Y.Q. Zhao, C.G. Wang, Y.J. Bai, G.W. Chen, M. Jing, B. Zhu, Property changes of powdery polyacrylonitrile synthesized by aqueous suspension polymerization during heat-treatment process under air atmosphere, *J. Colloid Interf. Sci.* 329 (2009) 48-53.
28. A.K. Gupta, D.K. Paliwal, P. Bajaj, Effect of an acidic comonomer on thermooxidative stabilization of polyacrylonitrile, *J. Appl. Polym. Sci.* 58 (1995) 1161-1174.
29. W.N. Turner, F.C. Johnson, The pyrolysis of acrylic fiber in inert atmosphere. I. Reactions up to 400°C, *J. Appl. Polym. Sci.* 13 (1969) 2073-2084.
30. Y. Tsuchiya, K. Sumi, Thermal decomposition products of polyacrylonitrile, *J. Appl. Polym. Sci.* 21 (1977) 975-980.
31. O.P. Bahl, R.B. Mathur, K.D. Kundra, Structure of PAN fibres and its relationship to resulting carbon fibre properties, *Fibre Sci. Technol.* 15 (1981) 147-151.

32. T.H. Ko, P. Chiranairadul, H.Y. Ting, C.H. Lin, The effect of modification on structure and dynamic mechanical behavior during the processing of acrylic fiber to stabilized fiber, *J. Appl. Polym. Sci.* 37 (1989) 541-552.
33. M.J. Yu, Y.J. Bai, C.G. Wang, Y. Xu, P.Z. Guo, A new method for the evaluation of stabilization index of polyacrylonitrile fibers, *Mater. Lett.* 61 (2007) 2292-2294.
34. P. Bajaj, M. Padmanaban, Copolymerization of Acrylonitrile with 3-chloro, 2-hydroxy-propyl acrylate and methacrylate, *J. Polym. Sci. Polym. Chem.* 21 (1983) 2261-2270.
35. T. Usami, T. Itoh, H. Ohtani, S. Tsuge, Structural study of polyacrylonitrile fibers during oxidative thermal degradation by pyrolysis-gas chromatography, solid-state carbon-13 NMR, and Fourier-transform infrared spectroscopy, *Macromolecules* 23 (1990) 2460-2465.
36. S.B. Deng, R.B. Bai, J.P. Chen, Behaviors and mechanisms of copper adsorption on hydrolyzed polyacrylonitrile fibers, *J. Colloid Interf. Sci.* 260 (2003) 265-272.
37. M. Minagawa, K. Miyano, M. Takahashi, Infrared characteristic absorption bands of highly isotactic poly(acrylonitrile), *Macromolecules* 21 (1998) 2387-2391.